


The CC-NB-LRR OsRLR1 mediates rice disease resistance through interaction with OsWRKY19

Dan Du^{1,†}, Changwei Zhang^{1,†}, Yadi Xing^{1,3}, Xin Lu¹, Linjun Cai¹, Han Yun¹, Qiuli Zhang¹, Yingying Zhang¹, Xinlong Chen¹, Mingming Liu¹, Xianchun Sang¹, Yinghua Ling¹, Zhenglin Yang¹, Yunfeng Li¹, Benoit Lefebvre^{1,2} and Guanghua He^{1,*} 

¹Key Laboratory of Application and Safety Control of Genetically Modified Crops, Academy of Agricultural Sciences, Rice Research Institute, Southwest University, Chongqing, China

²LIPM, INRAE, CNRS, Université de Toulouse, Castanet-Tolosan, France

³Agricultural College, Zhengzhou University, Zhengzhou, China

Received 24 February 2020;

accepted 7 December 2020.

*Correspondence (Tel +86 023 68250158;

fax 023 68250158; email:

heghswu@163.com)

[†]These authors contributed equally to this work.

Keywords: NB-LRR, *OsRLR1*, *OsWRKY19*, *Pyricularia oryzae* (syn. *Magnaporthe oryzae*), *Xanthomonas oryzae* pv. *oryzae* (Xoo), rice.

Summary

Nucleotide-binding site–leucine-rich repeat (NB-LRR) resistance proteins are critical for plant resistance to pathogens; however, their mechanism of activation and signal transduction is still not well understood. We identified a mutation in an as yet uncharacterized rice coiled-coil (CC)-NB-LRR, *Oryza sativa* *RPM1*-like resistance gene 1 (*OsRLR1*), which leads to hypersensitive response (HR)-like lesions on the leaf blade and broad-range resistance to the fungal pathogen *Pyricularia oryzae* (syn. *Magnaporthe oryzae*) and the bacterial pathogen *Xanthomonas oryzae* pv. *oryzae*, together with strong growth reduction. Consistently, *OsRLR1*-overexpression lines showed enhanced resistance to both pathogens. Moreover, we found that *OsRLR1* mediates the defence response through direct interaction in the nucleus with the transcription factor *OsWRKY19*. Down-regulation of *OsWRKY19* in the *rlr1* mutant compromised the HR-like phenotype and resistance response, and largely restored plant growth. *OsWRKY19* binds to the promoter of *OsPR10* to activate the defence response. Taken together, our data highlight the role of a new residue involved in the NB-LRR activation mechanism, allowing identification of a new NB-LRR downstream signalling pathway.

Introduction

Plants have developed sophisticated and inducible defence mechanisms against pathogen attack that involves recognition of and response to pathogen molecules at the plant cell surface or within the cell by host receptors. The plant pattern-recognition receptors recognize conserved microbe-associated molecular patterns (MAMPs) at the cell surface to stimulate MAMP-triggered immunity (MTI), which functions as the basal defence response in plants (Jones and Dangl, 2006; Tena *et al.*, 2011). To interfere with plant MTI, pathogens produce virulence effectors that can be recognized directly or indirectly by a host resistance (R) protein. Successful recognition between pathogen effector and R protein can trigger effector-triggered immunity (ETI) in plants to prevent the forward colonization of pathogens (Dodds and Rathjen, 2010; Jones and Dangl, 2006). Activation of ETI often causes strong accumulation of reactive oxygen species (ROS) and cell death at infected sites, termed hypersensitive response (HR). The activation of both MTI and ETI can result in activation of systemic acquired resistance (SAR), which enhances the overall degree of resistance to plant diseases (Jones and Dangl, 2006).

The classic ‘gene-for-gene’ concept of ETI in plants (Hammond-Kosack and Jones, 1997) proposes a receptor–ligand model

with a higher degree of complexity, where a plant R protein recognizes an avirulence (Avr) protein directly or indirectly by detecting effector-mediated modification of host proteins to initiate the defence response (Mackey *et al.*, 2002; Mestre and Baulcombe, 2006). R proteins that contain a nucleotide-binding domain (NB) and apoptosis APAF-1 and CED-4 conserved domain (ARC) and C-terminal leucine-rich repeats (LRR) are known as NB-LRR receptors, hereafter NLRs. NLRs can be divided into two broad classes on the basis of their N-terminal domains, which shows homology to the *Drosophila* Toll protein and mammal interleukin-1 receptor, and is known as Toll/interleukin-1 receptor (TIR) or be a coiled-coil (CC) domain (Monosi *et al.*, 2004). These are termed TIR-NB-LRR (TLRs) and CC-NB-LRR (CLRs), respectively. Generally, the CC domain of CLRs is required for association with accessory proteins, which is vital for downstream signalling (Lukasik and Takken, 2009; Swiderski *et al.*, 2009). The CC domain can activate a defence response cascade through association with WRKY transcription factors. Over- or ectopic-expression of this domain alone often causes localized cell death (Cheng *et al.*, 2015; Hu *et al.*, 2017; Inoue *et al.*, 2013). The NB-ARC domain predominantly participates in nucleotide binding, and strong conformational changes in this domain are associated with exchange between ADP and ATP (Takken *et al.*, 2006; Tameling *et al.*, 2002). Many conserved motifs have been

identified in this region. The P-loop (Walker A or kinase 1a motif) and Walker B are two conserved motifs of P-loop NTPases (Tameling *et al.*, 2006), mutation of which commonly causes loss of function of the NLR protein (Lolle *et al.*, 2017). Mutation of other conserved motifs, such as RNBS-A, RNBS-D and MHD, may cause effector-independent conformational changes that result in autoactivation or loss of function of NLR proteins (Mestre and Baulcombe, 2006; Tameling *et al.*, 2006; Zhang *et al.*, 2003). The LRR domain is relatively diverse and predominantly functions in the recognition of effectors (Shen *et al.*, 2003).

In the absence of effectors, the NLRs are in an ADP-bound state in which intra-molecular interactions maintain the proteins inactive; in the presence of effectors, conformational changes associated with the ATP-bound state lead to disruption of the repressive intra-molecular interactions and exposition of the N-terminal domain (CC or TIR), allowing remodelling of signal complexes (Mestre and Baulcombe, 2006; Sukarta *et al.*, 2016). Autoimmunity caused by mutation of NLRs often causes stunted growth and development of plants, accumulation of reactive oxygen species, elevated expression of defence-related genes and lesion-like cell death in the leaves (De Oliveira *et al.*, 2016; Grant *et al.*, 2000; Zhang *et al.*, 2003). In-depth analysis showed that dimerization of invariant CLRs in a CC domain-dependent manner is a minimal functional unit in immune signalling (Maekawa *et al.*, 2011). Forward studies revealed that the CC or TIR domains of NLRs formed a homo- or heteromeric complex that was associated with a chaperone and one or more WRKYs simultaneously to activate the downstream signal (Maekawa *et al.*, 2011; Shirasu, 2009; Tran *et al.*, 2017).

NLRs participate in defence responses to multiple pathogens, such as fungi, bacteria, viruses and insects. In rice, although considerable numbers of NLR genes have been identified and studied to elucidate the mechanism of immunity mainly against pathogens such as *Pyricularia oryzae* (syn. *Magnaporthe oryzae*), *Xanthomonas oryzae* pv. *oryzae* (Xoo) and *Rhizoctonia solani*, previous studies have typically focused on resistance to a single pathogen, especially the fungal pathogen *P. oryzae*, and only a limited number of reports have concentrated on two or more pathogens in rice (Chen and Ronald, 2011; Li *et al.*, 2019). Associated with one of the most devastating diseases in cultivated rice, the rice blast, *P. oryzae* infects epidermal cells by generating specialized appressorium and spreads biotrophically in plant cells (Wilson and Talbot, 2009). *X. oryzae* are agents of bacterial blight and leaf streak in rice, possessing type III secretion system for self multiplication and promotion of pathogenicity in host plants (Timilsina *et al.*, 2020). The fungal pathogen *R. solani*, the agent of the rice sheath blight, developed a necrotrophic means of colonizing and spreading, leading to considerable research on the pathogenesis involved (Molla *et al.*, 2020). Among the cloned NLRs in rice, the most intensively studied protein is BPH14, which is associated with two transcription factors, OsWRKY46 and OsWRKY72, which bind to the promoter of *RLCK281* and a callose synthase gene to mediate insect resistance (Hu *et al.*, 2017). In the present study, we identified a CLR protein, named OsRLR1 due to its high homology to RPM1 in *Arabidopsis thaliana*. RPM1, first identified in 1995, conducts recognition of two effectors: *avrRpm1* and *avrB* from the bacteria *Pseudomonas syringae* (Grant *et al.*, 1995; Mackey *et al.*, 2002). Mutation and overexpression of *OsRLR1* conferred resistance to the fungal pathogen *P. oryzae* and the bacterial pathogen Xoo. OsRLR1 associated with the transcription factor OsWRKY19 to regulate defence in rice.

Results

Point mutation in the NLR OsRLR1 induces spontaneous HR-like lesions

From a rice mutant library subjected to EMS treatment, we identified a recessive mutant, *rlr1* (previously designated *lmes2*), that developed HR-like lesions on the leaf blade with an early senescence phenotype in the absence of pathogen infection (Xing *et al.*, 2016). We previously mapped the mutation in a 66-kb interval on chromosome 10 (Xing *et al.*, 2016). We sequenced all genes in this interval and found a single-base transversion (A to T) at the 953 bp site of the coding sequence in *LOC_Os10g07978*, causing an amino acid change from Glu to Val at position 318 in the protein (Figure 1a). The single exon of *LOC_Os10g07978* encodes a 923 amino acid protein. A BLASTP search of the NCBI database (<https://blast.ncbi.nlm.nih.gov/Blast.cgi>) revealed that the most similar homolog of *LOC_Os10g07978* is the CLR from *Arabidopsis thaliana* RPM1 (33% identity and 52% similarity). Thus, *LOC_Os10g07978* was a putative homolog of *RPM1* and the gene was designated *Oryza sativa RPM1-like resistance gene 1* (*OsRLR1*). As RPM1, OsRLR1 is a typical CLR protein with N-terminal CC domains (32–165), NB domain (178–330), ARC domain (331–523) and the C-terminal LRR domain (551–923). The mutation was located in the NB domain and caused a change from the hydrophilic, polar negatively charged amino acid Glu to the nonpolar hydrophobic amino acid Val (Figure 1b).

To verify that *OsRLR1* is the gene causing the phenotype, we cloned the coding sequence of *LOC_Os10g07978* from the wild type (WT) and overexpressed it in *rlr1* plants. We sequenced the mutated site in the WT, *rlr1* mutant and T₀ transgenic plants. Only the transgenic plants were polymorphic at the mutation site (both A and T), which confirms that the transformation was successful (Figure S1a). The transcript level of *OsRLR1* was much higher in the homozygous T₂ transgenic plants than in the WT or *rlr1* mutant plants (Figure 1c). The transgenic plants recovered a phenotype similar to that of the WT (Figure 1d–e). At the same time, overexpressing mutated OsRLR1 (E318V, thereafter called OsRLR1_M) in the WT showed the HR-like phenotype on the leaf blade like *rlr1* (Figure S1b–c). We also measured the transcript levels of pathogenesis-related (PR) genes *OsPR1a* and *OsPR10*, two marker genes of immunity activation. The expression levels of the two genes were elevated significantly (Figure S1d). These results show that the mutation in *OsRLR1* (*LOC_Os10g07978*) accounted for the *rlr1* phenotype. Considering the role of CLRs in immunity, we analysed the disease resistance/susceptibility of the WT, *rlr1* mutant and the transgenic lines. At 10 dpi for *P. oryzae*, the lesion length and lesion number in the *rlr1* leaf blades were considerably shorter and lower, respectively, than that seen in the WT and transgenic plants (Figure 1f–h). Similarly, at 15 dpi for Xoo, the lesion length and bacterial population were considerably reduced in the *rlr1* mutant compared with the WT and transgenic plants (Figure 1i–k). In contrast, no notable difference was observed between the WT and *rlr1* mutant plants in the lesions caused by the fungal *R. solani* (Figure S1e, f).

To explore the function of *OsRLR1*, its basal expression pattern and subcellular localization were analysed. Results of qRT-PCR show that *OsRLR1* is mainly expressed in leaf blades (Figure S1g). A 3484 bp sequence of the *OsRLR1* promoter was cloned in transcriptional fusion with the *GUS* gene. GUS staining of *ProOsRLR1::GUS* transgenic plants shows that *OsRLR1* was mainly expressed in the vascular bundles of the leaf blade (Figure S1h, i).

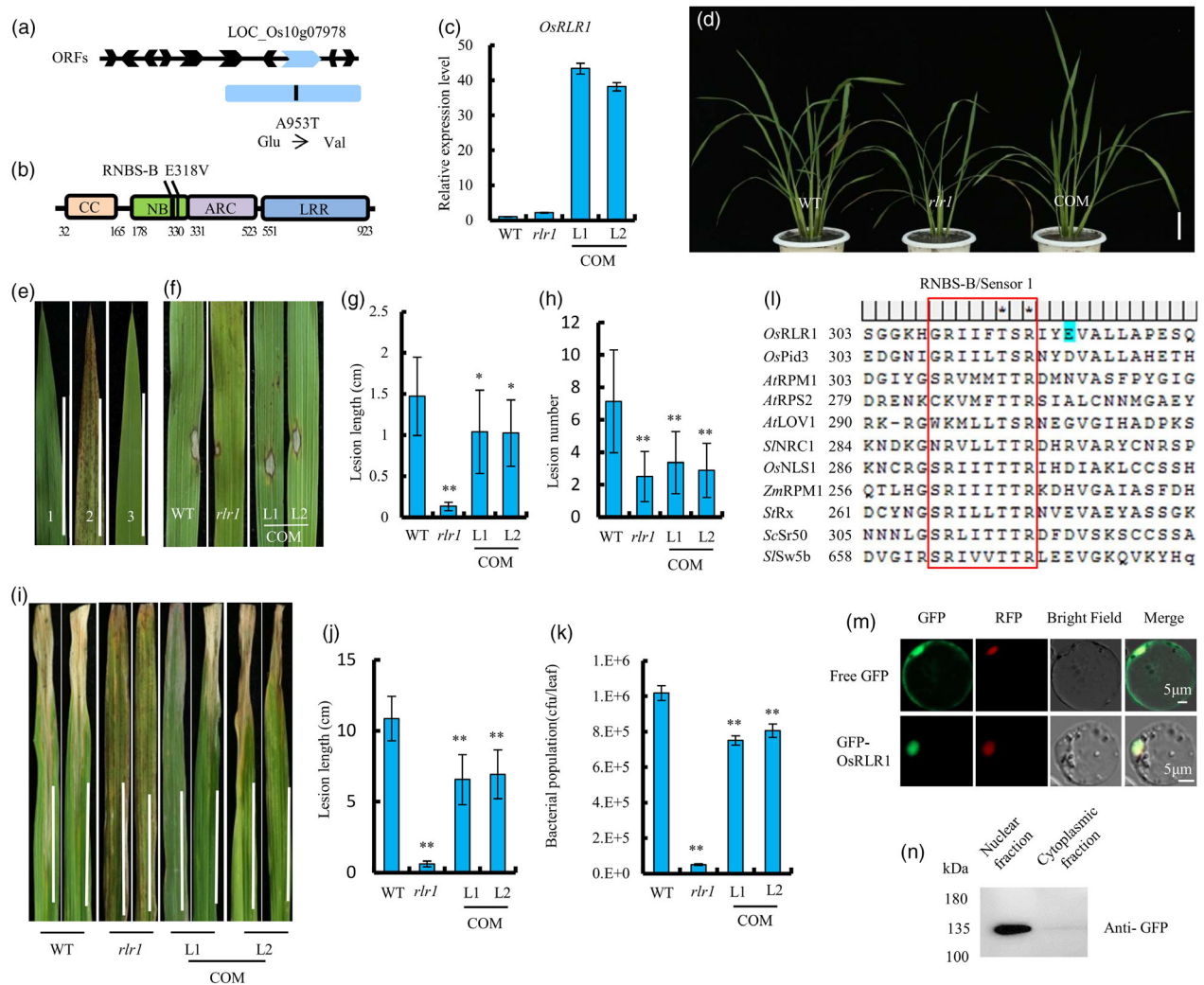


Figure 1 Point mutation in the CLR *OsRLR1* leads to broad-range resistance against pathogens. (a) Genes in previously mapped *lmes2* region and the mutation site of *OsRLR1*; blue box represents the *OsRLR1* open reading frame, and black line represents the mutation site. (b) Schematic diagram of *OsRLR1* protein structure. (c) Relative expression level of *OsRLR1* in WT, *rlr1* mutant and complementation lines (COM; *rlr1* mutant line transformed with *ProUbi::OsRLR1*); values represent means \pm SD ($n = 3$). L1 and L2 represent individual COM lines. (d) Images of plants at tillering stage. Bar = 5 cm. (e) Leaves of WT (1); *rlr1* mutant (2); and COM (3). (f) Diseased leaves at 10 days after *P. oryzae* inoculation. (g) Lesion length at 10 days after *P. oryzae* inoculation ($n = 30$). (h) Lesion number of the whole leaf blade at 10 days after *P. oryzae* inoculation ($n = 30$). (i) Diseased leaves at 15 days after *Xoo* inoculation. (j) Lesion length at 15 days after *Xoo* inoculation ($n = 15$). (k) *Xoo* population in inoculated leaves at 15 days after inoculation ($n = 3 \times 5$). (l) Sequence alignment of *OsRLR1* and other CLR proteins; the mutated amino acid is highlighted in blue. (m) Co-localization of *OsRLR1*-GFP with a nucleus-localized RFP in rice protoplast; free GFP was used as control (upper row). (n) Immunodetection of *OsRLR1*-GFP after cell fractionation of *N. benthamiana* leaves. * $P < 0.05$; ** $P < 0.01$ (Student's *t*-test).

When *OsRLR1*-GFP and nuclear marker-RFP were co-expressed in rice protoplasts, the green and red fluorescent protein (RFP) signals were superimposed (Figure 1m). Western blot showed that the *OsRLR1*-GFP fusion protein was in the nuclear fraction after cell fractionation (Figure 1n). These results indicate that *OsRLR1* exerts its biological function in the nucleus.

A multiple sequence alignment of *OsRLR1* and reported CLRs from rice, Arabidopsis, tomato, potato, maize and wheat was generated (accession numbers are listed in Table S2). The mutated amino acid was located close to a relatively conserved motif, RNBS-B/sensor 1, in the NB domain (Figure 1l). Nineteen CLRs from an additional 10 species were included in the alignment for phylogenetic analysis. *OsRLR1* was clustered with the rice blast resistance protein PID3, *A. thaliana* RPM1 and

ZmRPM1 (Figure S1j). Taken together, these results suggest that *OsRLR1* may function as a typical CLR gene involved in the disease resistance pathway in rice.

OsRLR1 positively regulates defence responses

To examine the role of *OsRLR1* in the defence response, we overexpressed *OsRLR1* in the WT. Three *OsRLR1* overexpression homozygous transgenic T₂ (*OsRLR1*-OX) lines were obtained. At the tillering stage, the expression level of *OsRLR1* in the three *OsRLR1*-OX lines was more than 100 times that of the WT (Figure 2a). At this stage, *OsRLR1*-OX plant growth was similar to the WT. In contrast to the *rlr1* mutant line, no HR-like lesions were observed on the leaf blades of the *OsRLR1*-OX lines (Figure S2a-f). Moreover, overexpression of *OsRLR1* had no

significant influence on the agronomic traits of the *OsRLR1*-OX lines (Figure S2g).

We inoculated the WT, *rlr1* mutant and the three *OsRLR1*-OX lines with *P. oryzae*. The lesion length and lesion number at 10 dpi in the *OsRLR1*-OX plants were significantly reduced compared with the WT (Figure 2b–d). The same lines were also inoculated with *Xoo*. The lesion length was measured at 5, 10 and 15 dpi. The *OsRLR1*-OX lines developed a shorter lesion than the WT at all time points (Figure 2e,f). Consistently, the bacterial population in the WT was larger than that in the *OsRLR1*-OX lines at 15 dpi (Figure 2g). Therefore, *OsRLR1* positively regulates defence resistance in rice.

Leaf blades were sampled at 0, 3, 12, 24, 48, 72 and 96 hours post-inoculation (hpi) with *P. oryzae*. At all time points, the expression level of *OsRLR1* in the transgenic lines was much higher than that in the WT, which confirmed that the transformation was successful (Figure 3a). We also measured the

transcript levels of *OsNPR1*, an immunity regulator and the *PR* genes *OsPR1a* and *OsPR10*. The expression levels of the three genes were significantly higher in the *OsRLR1*-OX and in the *rlr1* mutant plants than in the WT at almost all time points (Figure 3a). These results indicate that an enhanced defence response was activated by *P. oryzae* infection both in the *rlr1* mutant lines and in *OsRLR1*-OX lines. A similar trend was observed at 5 and 10 dpi with *Xoo* (Figure 3b). Taken together, these results show that *OsRLR1* positively regulates defence response in rice.

OsRLR1 interacts with OsWRKY19

Given that CLRs often function in the defence response in association with WRKY transcription factors, five defence-related WRKY proteins (*OsWRKY13*, *OsWRKY19*, *OsWRKY47*, *OsWRKY68* and *OsWRKY76*) were screened for ability to interact with the CC domain of OsRLR1 (*OsRLR1_{CC}*) using a yeast two-hybrid system. The full-length WRKY proteins often auto-activate

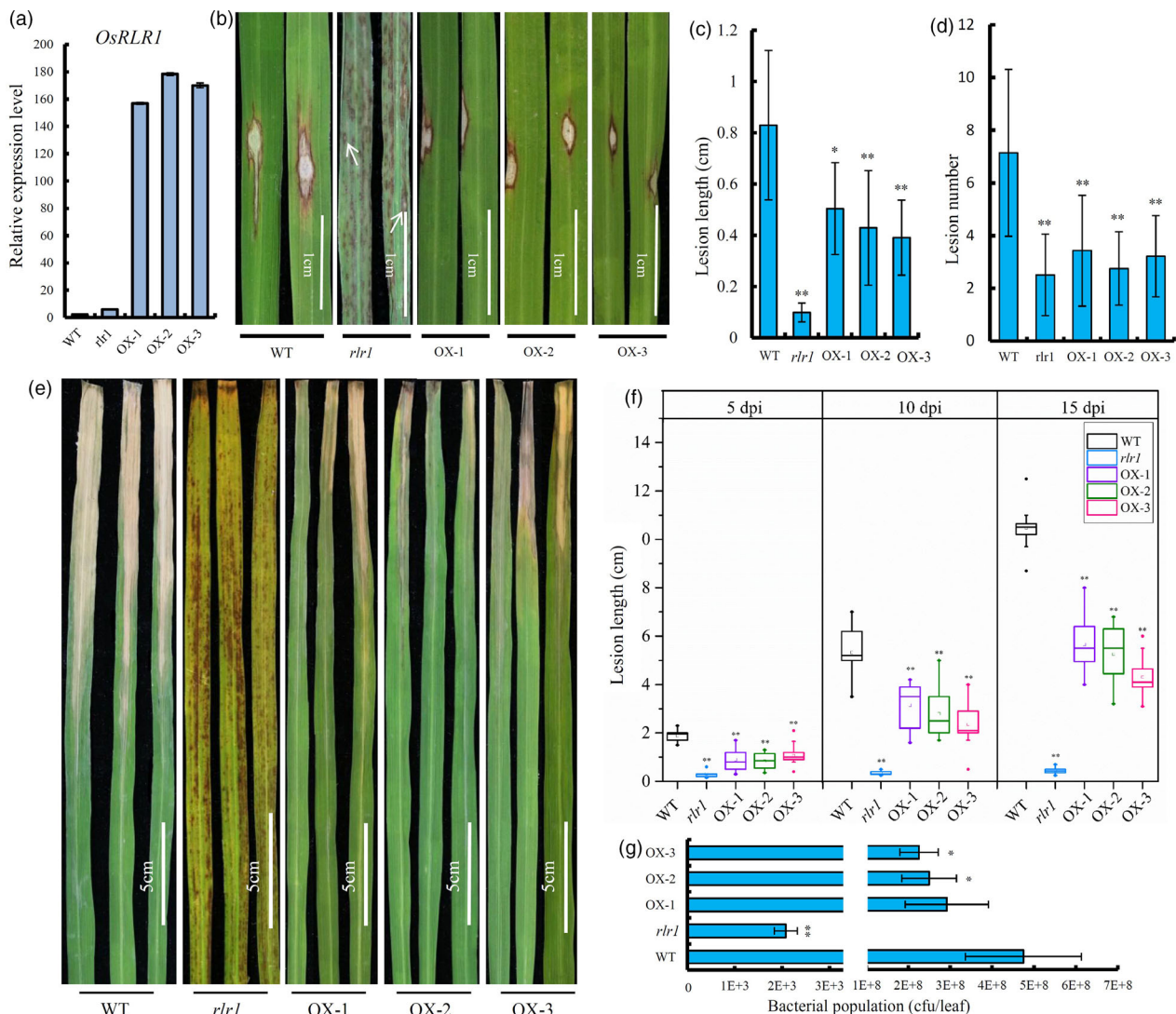


Figure 2 *OsRLR1* positively regulates the defence responses. (a) Relative expression level of *OsRLR1* in WT, *rlr1* mutant and *OsRLR1*-overexpressing lines in the WT background (*OsRLR1*-OX); values represent means \pm SD ($n = 3$). (b) Diseased leaves at 10 days post-inoculation (dpi) with *P. oryzae*. (c) Lesion length of diseased leaves at 10 dpi with *P. oryzae* ($n = 30$). (d) Lesion number of the whole leaf blade at 10 dpi with *P. oryzae* ($n = 30$). (e) Diseased leaves at 15 dpi with *Xoo*. (f) Lesion length of diseased leaves at 5, 10 and 15 dpi with *Xoo* ($n = 15$). (g) Bacterial population in inoculated leaves at 15 dpi with *Xoo* ($n = 3 \times 5$). * $P < 0.05$; ** $P < 0.01$ (Student's *t*-test).

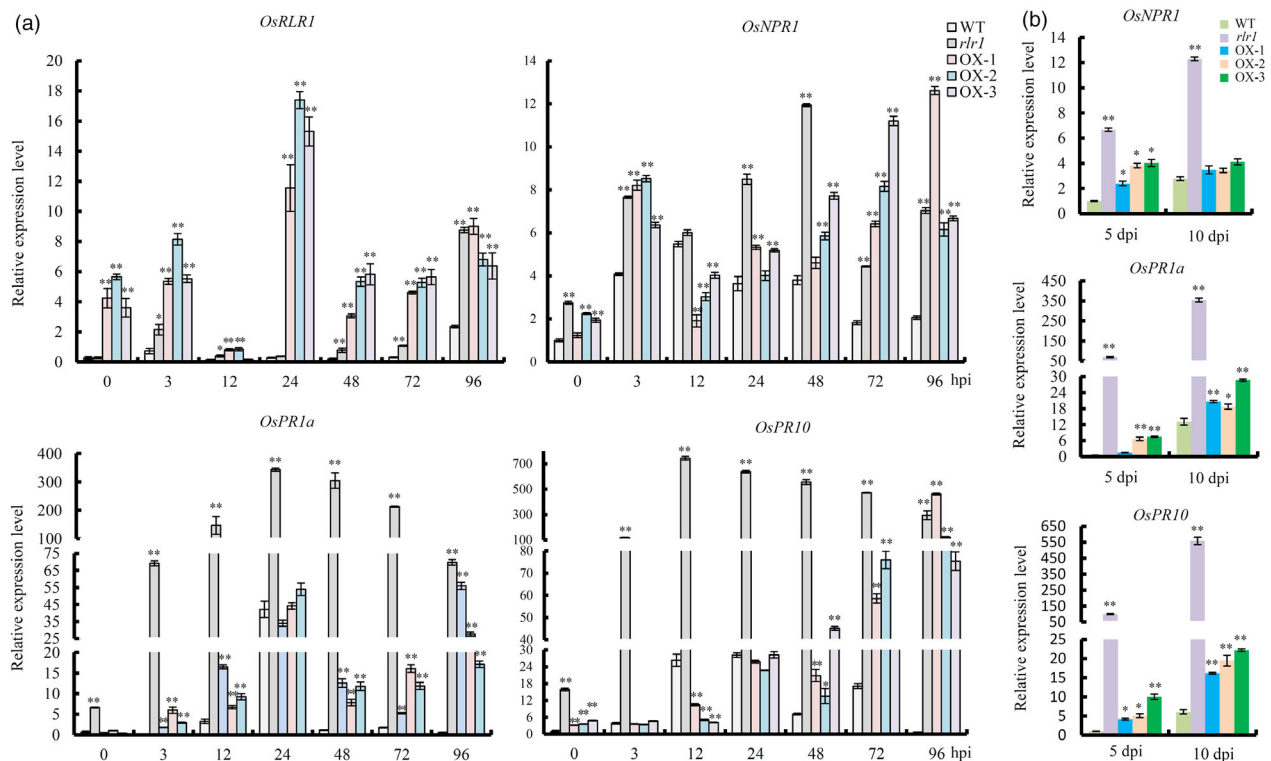


Figure 3 Defence-related gene expression in *OsRLR1*-OX lines after *P. oryzae* and *Xoo* inoculation. (a) Relative expression level of *OsRLR1*, *OsNPR1*, *OsPR1a* and *OsPR10* in the WT, *rlr1* mutant and three *OsRLR1*-OX lines at 0, 3, 12, 24, 48, 72 and 96 h post-inoculation (hpi) with *P. oryzae*; values represent means \pm SD ($n = 3$). (b) Relative expression level of *OsNPR1*, *OsPR1a* and *OsPR10* in WT, *rlr1* and three *OsRLR1*-OX lines at 5 and 10 dpi with *Xoo*; values represent means \pm SD ($n = 3$). * $P < 0.05$; ** $P < 0.01$ (Student's *t*-test).

the Y2H system (Inoue *et al.*, 2013); hence, truncated proteins were used in this study. All co-transformed yeasts grew on DDO medium (Figure 4a left), whereas only *OsWRKY19* interacted with *OsRLR1_{CC}* to allow growth on QDO/AbA medium (Figure 4a right). For further characterization of the interaction, truncated and full-length *OsRLR1* and *OsRLR1_M* proteins were each expressed with *OsWRKY19* into yeast. All co-transformed yeasts grew on DDO medium (Figure 4b left). All truncated *OsRLR1* and *OsRLR1_M* lacking the LRR domain, but not the full-length *OsRLR1* nor *OsRLR1_M*, interacted with *OsWRKY19* (Figure 4b right). In addition, in the Y2H system, the *OsRLR1* CC domain, but not the NB, ARC, or LRR domains, formed self-association (Figure S3).

In rice protoplasts, the GFP signal of the *OsWRKY19*-GFP fusion protein co-localized with the RFP signal of the nuclear marker protein, while the free GFP was observed both in cytoplasm and nucleus (Figure S5a). The *OsWRKY19*-GFP fusion protein was detected by Western blot in the nuclear fraction after cell fractionation (Figure S5b). In *Nicotiana benthamiana* leaves, the GFP fluorescence of *OsRLR1*-GFP, *OsRLR1_M*-GFP and *OsWRKY19*-GFP was also localized in the nucleus as labelled by DAPI (Figure S5c). We next verified the interaction between *OsRLR1* and *OsWRKY19* *in planta* using a bimolecular fluorescence complementation (BiFC) assay. The YFP fluorescence was observed in the nucleus of *N. benthamiana* leaves that co-expressed *OsRLR1*-cYFP and *OsWRKY19*-nYFP (Figure 4c). Similar YFP fluorescence in the nucleus was observed when *OsRLR1_M*-cYFP and *OsWRKY19*-nYFP were co-expressed (Figure 4c). A co-immunoprecipitation assay (Figure 4d) and a split *LUC* assay (Figure 4e,f) confirmed that *OsRLR1* and *OsRLR1_M* interacted

with *OsWRKY19* in *N. benthamiana* leaves. Thus, both *OsRLR1* and *OsRLR1_M* interacted with *OsWRKY19* in the nucleus.

The results described above suggest that *OsWRKY19* participates in the *OsRLR1*-mediated defence response. Consistent with this conclusion, we found that *OsWRKY19* was up-regulated in *OsRLR1*-OX and in *rlr1* plants at almost all sampling time points after inoculation with *P. oryzae* (Figure S6).

OsWRKY19 mediates *OsRLR1*-induced defence responses

To explore further the role of *OsWRKY19* in the *OsRLR1*-mediated resistance response, we used RNAi to silence *OsWRKY19* in *rlr1*. The *OsWRKY19* expression level in all T_0 transgenic lines was less than that in *rlr1* (Figure 5a). The phenotype of the *rlr1* *OsWRKY19*-silenced plants (*rlr1* *OsWRKY19_{RNAi}*) was assessed in T_2 plants. At the tillering stage, compared with *rlr1* plants, the growth and development of *rlr1* *OsWRKY19_{RNAi}* plants were better, although not comparable to WT plants (Figure 5b–d). The first, second and third youngest leaves of *rlr1* *OsWRKY19_{RNAi}* plants developed fewer HR-like lesions than *rlr1* plants (Figure 5e–g). The DAB staining of the second and third leaves indicates that H_2O_2 accumulation was reduced in *rlr1* *OsWRKY19_{RNAi}* plants compared with *rlr1* plants, while almost no H_2O_2 was detected in the WT (Figure 5h). At the maturity stage, *rlr1* *OsWRKY19_{RNAi}* plants were considerably taller and developed a greater number of tillers (Figure 5i), longer ears and more grains (Figure 5j) than *rlr1* plants. Agronomic trait analysis of the *rlr1* *OsWRKY19_{RNAi}* line that showed the best development reveals that all traits were significantly increased compared with the *rlr1* mutant although not restored to the level of the WT (Figure S7a–h).

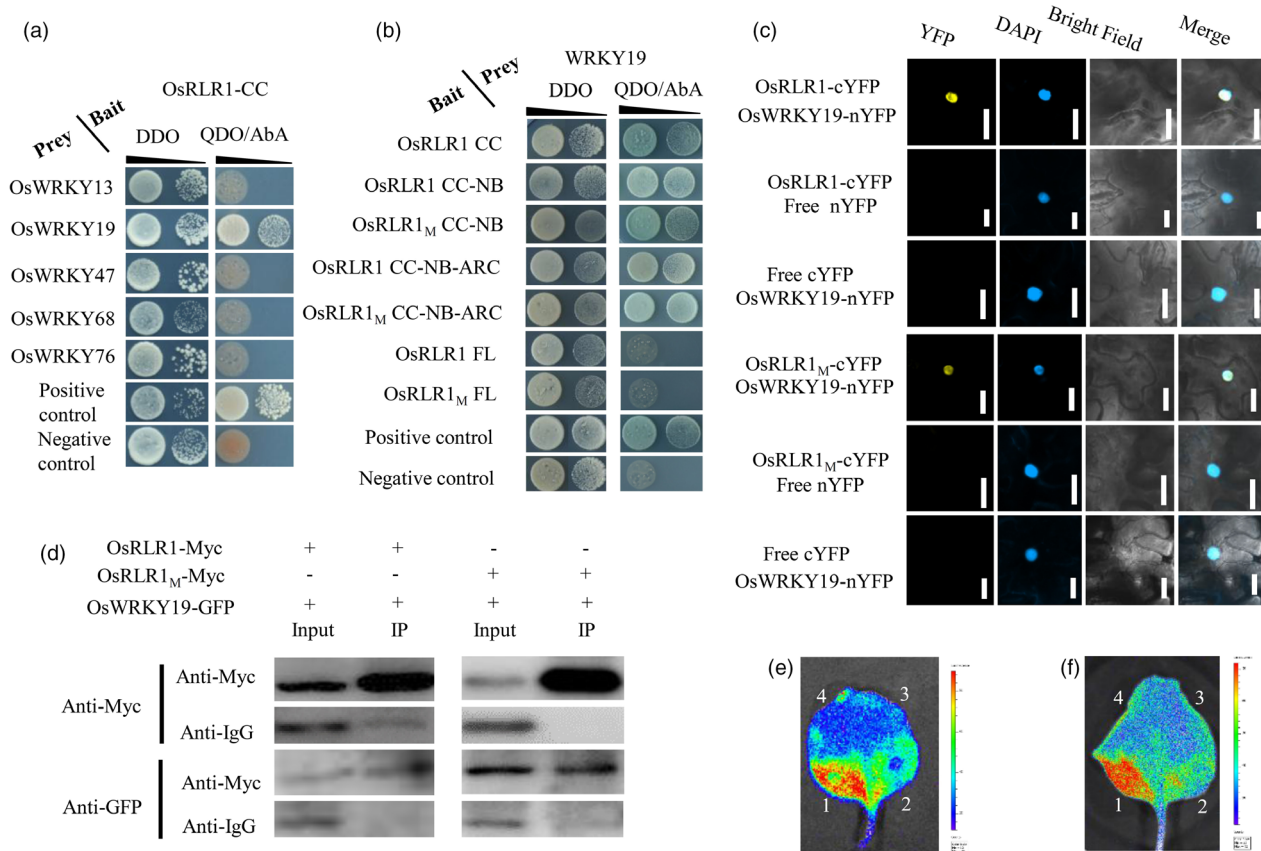


Figure 4 OsRLR1 interacts with OsWRKY19. (a) Yeast two-hybrid (Y2H) assay between OsRLR1 CC domain and several rice WRKY proteins. (b) Y2H assay between truncated OsRLR1 and OsWRKY19 proteins. (c) Bimolecular fluorescence complementation (BiFC) between OsRLR1-cYFP or OsRLR1_M-cYFP and OsWRKY19-nYFP in *Nicotiana benthamiana* leaves; nYFP and cYFP alone were used as negative controls. (d) Co-IP of OsRLR1-Myc with OsWRKY19-GFP (left) or OsRLR1_M-Myc with OsWRKY19-GFP (right). (e-f) Split luciferase assays. OsRLR1-Cluc (e) or OsRLR1_M-Cluc (f) was co-expressed with OsWRKY19-Nluc in *N. benthamiana* leaves. 1: OsRLR1-Cluc or OsRLR1_M-Cluc with OsWRKY19-Nluc; 2: OsWRKY19-Nluc with Cluc; 3: OsRLR1-Cluc or OsRLR1_M-Cluc with Nluc; and 4: Cluc with Nluc. Cluc and Nluc alone were used as negative controls.

Thus, the growth and development of *rlr1* OsWRKY19_{RNAi} plants were partially restored.

To determine whether silencing of *OsWRKY19* compromised the OsRLR1_M induced resistance to pathogens, WT, *rlr1* and *rlr1* OsWRKY19_{RNAi} plants were inoculated with *P. oryzae* at the four-leaf stage. The *rlr1* OsWRKY19_{RNAi} plants developed longer lesion length and larger lesion number compared with the *rlr1* mutant (Figure 6a,b,c). Similar results were observed after *Xoo* inoculation at the tillering stage (Figure 6d,e,f). Thus, down-regulation of *OsWRKY19* in the *rlr1* mutant weakened the OsRLR1_M-induced resistance to pathogens.

OsWRKY19 expression level in *P. oryzae*-inoculated leaves of two *rlr1* OsWRKY19_{RNAi} lines was significantly reduced compared with *rlr1* plants at all sampling time points, which shows that *OsWRKY19* silencing is maintained during *P. oryzae* infection (Figure S8a). In general, *OsRLR1* expression level in *rlr1* OsWRKY19_{RNAi} lines was reduced, but not at all time points (Figure S8b). *OsRLR1* expression is induced during the infection by *P. oryzae* (Figure 3a). It is also induced in the *rlr1* mutant, likely because a positive feedback regulation. It is thus coherent that its expression is decreased in the *rlr1* OsWRKY19_{RNAi} lines, in which signalling downstream OsRLR1 is decreased. Similarly, *OsNPR1* expression level was lower only at some time points after inoculation with *P. oryzae* and *Xoo* (Figure S8c,d). In contrast, the

expression levels of *OsPR1a* and *OsPR10* in *rlr1* OsWRKY19_{RNAi} plants were significantly decreased compared with those in *rlr1* plants at all time points (Figure 6g). Similar results were observed at 5 dpi with *Xoo* (Figure 6h). Thus, *OsWRKY19* contributes to OsRLR1-mediated defence responses in rice.

OsWRKY19 activates expression of *OsPR10*

To test the transcription activity of *OsWRKY19*, we used the luciferase (*LUC*) reporter system in rice protoplasts and found that expressing *OsWRKY19*-GAL4 BD enhanced *LUC* activity by a factor of more than 5 compared with the empty vector pGreenII800, which indicates that *OsWRKY19* functions as an active transcription factor (Figure 7a). Rice protoplasts that expressed *OsWRKY19* with *ProOsPR10*:*LUC* demonstrated enhanced *LUC* activity by a factor of 6 compared with the control transformed with *ProOsPR10*:*LUC* and the empty vector (Figure 7b), which indicates that *OsWRKY19* can activate the expression of *OsPR10*. To verify whether *OsWRKY19* can directly activate the expression of *OsPR10*, we analysed the promoter region of *OsPR10* using the PlantCARE database and detected four potential elements: three W-boxes and one WLE 1 (Figure 7c). CHIP assay was conducted *in vivo* using the WT and *rlr1* leaf blades at the seedling stage (Figure 7d,e). The results showed that for the sample IP with *OsWRKY19* antibodies from WT there

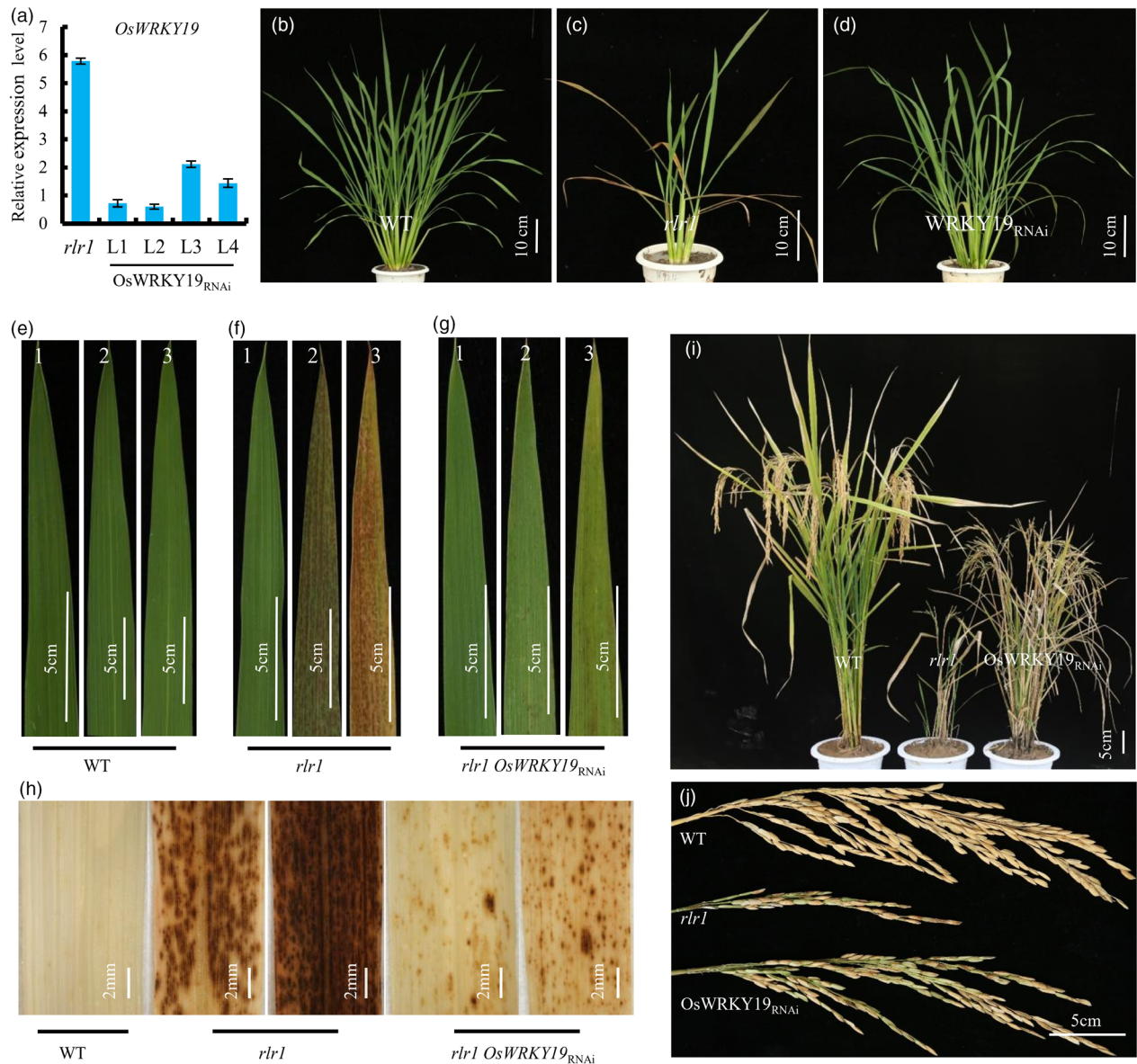


Figure 5 Spontaneous HR-like lesion phenotype of the *rlr1* mutant is compromised by silencing *OsWRKY19*. (a) Relative expression of *OsWRKY19* in *rlr1* *WRKY19*^{RNAi} T₀ plants; values represent means \pm SD ($n = 3$); L1-L4 are individual transgenic lines. (b–d) WT, *rlr1* mutant and homozygous T₂*rlr1* *WRKY19*^{RNAi} plants at the tillering stage. (e–g) Leaves of WT, *rlr1* and *rlr1 OsWRKY19*^{RNAi} plants; 1, 2 and 3 represent the first, second and third youngest leaves. (h) DAB staining of leaves of WT, *rlr1* and *rlr1 OsWRKY19*^{RNAi} plants; 2 and 3 represent the second and third leaves from the shoot apex. (i) WT, *rlr1* and *rlr1 WRKY19*^{RNAi} plants at the maturity stage. (j) Panicles of WT, *rlr1* and *rlr1 WRKY19*^{RNAi} plants at the maturity stage.

was slight enrichment of the PCR products using primers of sites P2 and P4, and significant enrichment of the PCR product using primers of site P3 (Figure 7d). In the *rlr1* mutant, sample IP with *OsWRKY19* antibodies showed significant enrichment of the PCR products at sites P2, P3 and P4 (Figure 7e). No PCR product in sample IP with *OsWRKY19* antibodies was detected using primers of site P1 in the WT or *rlr1* mutant (Figure 7d,e). Taken together, these results show that *OsWRKY19* may directly activate expression of *OsPR10*. Transactivation of *ProOsPR10:LUC* by *OsWRKY19* was also observed in *N. benthamiana* leaves. Interestingly, *LUC* activity was induced by co-expression of *OsRLR1* and even more by co-expression of *OsRLR1_M* (Figure 7f). These results suggest that interaction with *OsRLR1* facilitates the function of *OsWRKY19* in the activation of the *OsPR10* gene. These results

allow to propose a model of the defence response signal conduction from *OsRLR1* to *OsWRKY19* to *OsPR10* (Figure 7g).

Discussion

OsRLR1 is a typical CLR protein in rice

Resistance proteins are widely used by plants and mammals to aid recognition and response to pathogen attack by monitoring the presence of corresponding Avr proteins (Roberts *et al.*, 2013). The activation of R proteins upon recognition of an intruding pathogen commonly induces cell death at the intrusion site to disable pathogen growth and halt infection. Thus, in the absence of pathogens, R genes must be tightly and precisely regulated to avoid inappropriate activation. In *Arabidopsis*, RPM1 is located on

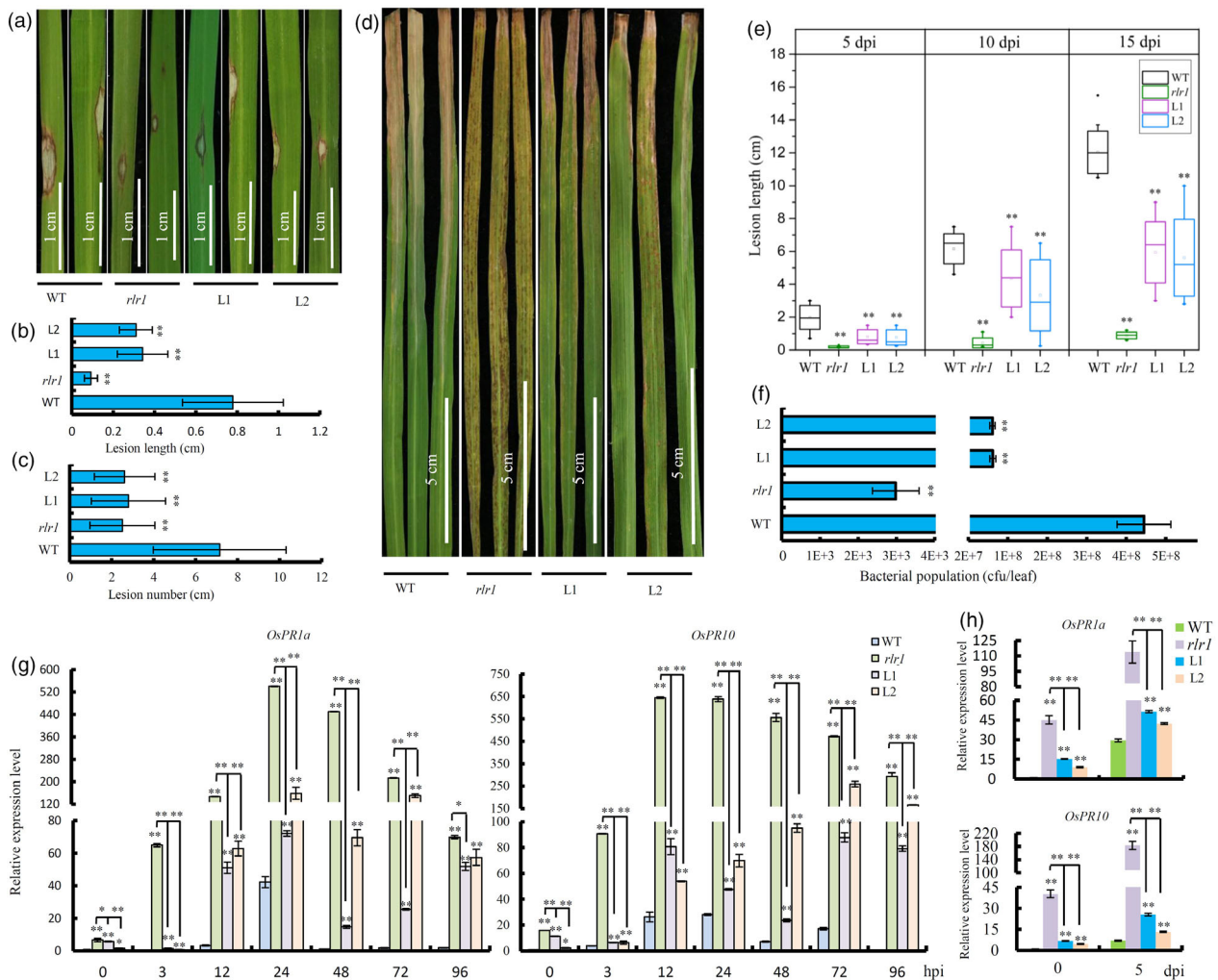


Figure 6 OsRLR1_M-induced resistance to *P. oryzae* and *X. oryzae* is compromised in silencing *OsWRKY19*. (a) Diseased leaves at 10 days post-inoculation (dpi) with *P. oryzae*. (b) Lesion length of diseased leaves at 10 dpi with *P. oryzae* ($n = 30$). (c) Lesion number of the whole leaf blade at 10 days after *P. oryzae* inoculation ($n = 30$). (d) Diseased leaves at 15 dpi with *Xoo*. (e) Lesion length of diseased leaves at 5, 10 and 15 dpi with *Xoo* ($n = 15$). (f) Bacterial population in inoculated leaves at 15 dpi with *Xoo* ($n = 3 \times 5$). (g) Relative expression level of *OsPR1a* and *OsPR10* in WT, *rlr1* mutant and *rlr1* WRKY19_{RNAi} plants at 0, 3, 12, 24, 48, 72 and 96 hpi with *P. oryzae*; values represent means \pm SD ($n = 3$). (h) Relative expression level of *OsPR1a* and *OsPR10* in WT, *rlr1* and *rlr1* WRKY19_{RNAi} plants at 5 dpi with *Xoo*. L1 and L2 represent individual lines of WRKY19_{RNAi} in *rlr1*. * $P < 0.05$; ** $P < 0.01$ (Student's *t*-test).

the peripheral plasma membrane and is repressed by a plasma membrane-localized protein, RIN4 (Boyes *et al.*, 1998; Mackey *et al.*, 2002). Phosphorylation of RIN4 caused by effectors from the bacterial pathogen *Pseudomonas syringae* can release RPM1 to trigger the ETI response (Mackey *et al.*, 2002). In the present study, we identified a rice *CLR* gene, *OsRLR1*, homologous to *RPM1*, which is expressed predominantly in vascular bundles of leaves. Unlike *RPM1*, *OsRLR1* is localized in the nucleus. Similarly to most *CLR*, for example *MLA10* in barley (Maekawa *et al.*, 2011) and *BPH14* in rice (Hu *et al.*, 2017), *OsRLR1* likely self-associates through its CC domain. Although *OsRLR1* cannot perceive the presence of the available Avr proteins directly (Figure S4), it cannot be excluded that *OsRLR1* may recognize effector in an indirect way. Point mutation and overexpression of *OsRLR1* increase resistance to the bacterial pathogen *Xoo* and fungal hemibiotroph pathogen *P. oryzae*. Interestingly, it does not increase resistance or susceptibility to the fungal necrotrophic pathogen *R. solani*, suggesting that *OsRLR1* controls specific

defence responses leading to resistance to biotrophic/ hemibiotrophic pathogens. Alternatively, we cannot exclude that *OsRLR1*-mediated immunity is active only in leaf blades and not in leaf sheaths.

Mutation of E318 in the NB domain leads to autoactivation of *OsRLR1*

Mutation in the RNBS-D domain in AtLOV1 (P437L) and *RPM1* (P442L) causes loss of function of the proteins (Sweat *et al.*, 2008), whereas mutation in StRx (E442L, close to RNBS-D) enables autoactivation of the protein (Bendahmane *et al.*, 2002). The *rlr1* mutant phenotype, including the leaf-tip necrosis, the strong ROS production and expression of *PR* genes in absence of pathogens as well as the ability of *OsRLR1*_M to induce *OsWRKY19* transcriptional activity in heterologous systems suggest that *OsRLR1*_M codes for an autoactive form of *CLR*. Mutation in the NB domain of two *CLR*s of tomato (*Solanum lycopersicum*), I-2 and Mi-1, impaired ATP hydrolysis and caused autoactivation

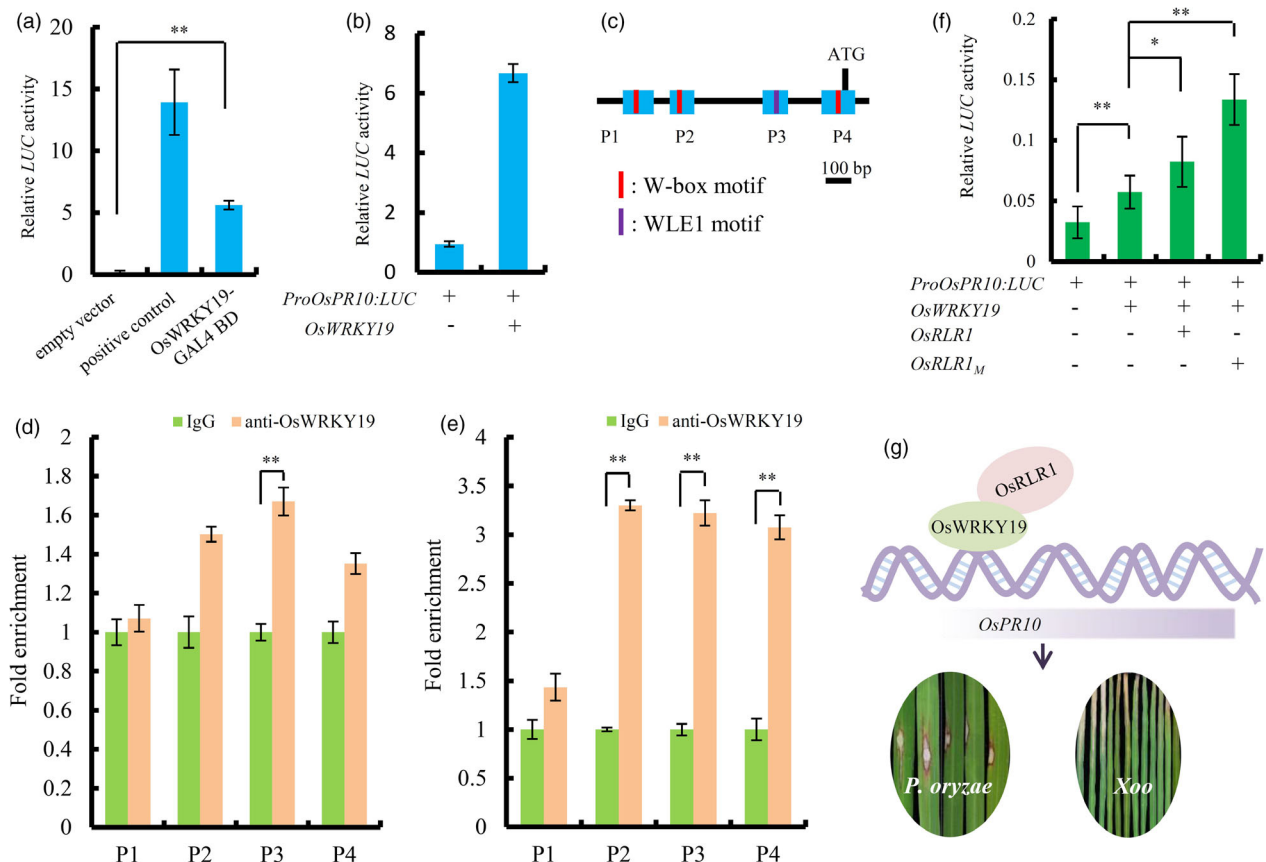


Figure 7 OsWRKY19 controls *OsPR10* expression. (a) Transcription factor activity assay. The empty vector *Pro35S::GAL*, and the positive control *Pro35S::GAL-VP16* or *Pro35S::OsWRKY19-GAL* construct were introduced in rice protoplasts. *LUC* activity was measured 12 h after protoplast transformation. (b) Transactivation assay in rice protoplasts. *LUC* activity was measured 12 h after transformation with the *Pro35S::OsWRKY19* and *ProOsPR10::LUC* constructs. (c) Distribution of potential binding sites in the promoter of *OsPR10*. Blue bars indicate the DNA fragments used for the CHIP assays; red lines indicate the W-box element and violet line indicates the WLE1 element. (d–e) CHIP-qPCR for P1–P4 sites of *OsPR10* promoter in wild type (d) and the *rlr1* mutant (e) was conducted using samples before IP (input) and after IP with anti-OsWRKY19 polyclonal antibodies or pre-immune IgG (control); values represent means \pm SD ($n = 3$). The presented qPCR results are ratios relative to the value of the IP sample with IgG. f: Transactivation assays in *N. benthamiana* leaves. *LUC* activity was measured 2 days after transformation with the *ProOsPR10::LUC*, *Pro35S::OsWRKY19*, *Pro35S::OsRLR1* and/or *Pro35S::OsRLR1_M*. (g): Proposed model for OsRLR1 and OsWRKY19 mediated defence response in rice. Minus (-) and plus (+) denote the presence or absence of the indicated constructs. * $P < 0.05$; ** $P < 0.01$ (Student's *t*-test).

(Tameling *et al.*, 2002; Tameling *et al.*, 2006). Modelling of the three-dimensional OsRLR1 structure revealed that the mutated site E318 is on the other face of the NB domain compared with the nucleotide-binding site (Figure S9c,d,e). Interestingly, the corresponding residue in AtZAR1, the only full-length plant NLR that has been crystallized to date (Wang *et al.*, 2019), is located outside the protein in the ADP-bound state (Figure S9a) and becomes extremely close to an α -helix of the ARC domain (Figure S9b) due to protein rearrangement, including a rotation of the NB domain in the ATP-bound state. Thus, the E318 or neighbouring residues of OsRLR1 may be involved in the stability of the protein in the ATP-bound state. The mutation OsRLR1_M might lock the tertiary structure corresponding to the activated state by altering the interaction between the NB and the ARC domains. Therefore, we speculate that the mutation in OsRLR1 might influence ATP hydrolysis either directly or indirectly. Many mutations in residues of the NB domain were found to lead to autoactivation of NLR (Figure S9, Table S3) (Bendahmane *et al.*, 2002; Tameling *et al.*, 2006; Tang *et al.*, 2011; Van Ooijen *et al.*, 2008); however, no previous study has reported that a mutation

close to the RNBS-B motif may cause autoactivation of an NLR. Thus, we have identified a new site that may be critical in NLR functioning.

OsRLR1 positively regulates the defence response in rice

NPR1 is vital in plant resistance. Mutation of *NPR1* in *Arabidopsis* abolishes expression of *PR* genes and completely compromises activation of SAR (Cao *et al.*, 1997), while overexpression of which enhanced pathogen resistance in a dose-dependent manner (Cao *et al.*, 1998). Overexpression of *OsNPR1* or *NH1* spontaneously activates the defence response and enables enhanced resistance to *Xoo* (Chern *et al.*, 2005). The higher expression level of *OsNPR1* and *PR* genes in both the *rlr1* and in the OsRLR1-OX plants, compared with the WT plants, suggests that OsRLR1 controls *OsNPR1* expression and consequently the *OsNPR1*-mediated defence response in rice. Expression of *PR* genes induces cell death to prevent pathogen growth at the invasion site (Sels *et al.*, 2008; Loon *et al.*, 2006). In the *rlr1* mutant, *OsPR1a* and *OsPR10* expressions were highly induced. This might account for massive cell death observed in the *rlr1*

mutant. Moreover, lower level of *OsPR1a* and *OsPR10* expression at 0 hpi in *OsRLR1*-OX lines than in the *rlr1* mutant line (Figure 3a,b) might explain the absence of HR-like lesions in *OsRLR1*-OX lines compared with the *rlr1* mutant line. Previous studies have shown that some NLR-mediated resistance is dosage-dependent (Howles *et al.*, 2005) and overexpression of NLR genes may result in autoactivity (Tao *et al.*, 2000). In the present study, *OsRLR1* overexpression in rice enhanced the defence response and led to broad-range resistance but caused neither an HR-like phenotype nor any effect on agronomic traits, which may encourage its potential use in enhancing disease resistance in rice breeding.

OsRLR1 functions with OsWRKY19 to regulate the defence response

WRKY transcription factors are specific to plants and algae, and play a variable role in developmental processes and biotic and abiotic stress responses (Cheng *et al.*, 2015; Devaiah *et al.*, 2007; Eulgem *et al.*, 2000). In plants, WRKY transcription factors often activate expression of *PR* genes by recognizing and binding to W-box or WLE 1 cis-regulatory elements (Choi *et al.*, 2015; Hu *et al.*, 2017; Inoue *et al.*, 2013). In rice, many WRKY proteins involved in pathogen resistance have been identified. The group II *OsWRKY62* is a negative regulator of rice resistance to *Xoo*, and its overexpression suppresses resistance by inhibiting the expression of defence-related genes (Peng *et al.*, 2008). In contrast, the group III *OsWRKY45* positively regulates defence responses to *P. oryzae* and *Xoo* but not to *R. solani* (Shimono *et al.*, 2012). The NLR protein *Pb1* mediates blast resistance in rice through interaction with *OsWRKY45* by the CC domain (Inoue *et al.*, 2013). In the present study, we found that *OsRLR1* interacts with *OsWRKY19* through the CC domain. As *OsWRKY45*, *OsWRKY19* belongs to group III of the WRKY family (Wang *et al.*, 2015; Xie *et al.*, 2005), which are predominantly responsive to pathogens and/or salicylic acid (Kalde *et al.*, 2003). *OsWRKY19*, activating the transcription of the *PR* gene, is a positive regulator of the defence response induced by *OsRLR1*. Down-regulation of *OsWRKY19* partially compromised the *OsRLR1_M*-mediated resistance to *P. oryzae* and *Xoo* and partially recovered the *OsRLR1_M*-mediated defective development. The partial recovery may be attributable to residual *OsWRKY19* expression in the *OsWRKY19*-silenced lines or to interaction of *OsRLR1* with other WRKY transcription factors that would have a redundant function in the defence response.

In conclusion, we have characterized a new rice CLR, *OsRLR1* and at least part of its downstream signalling pathway leading to defence activation. Moreover, we have identified a new residue E318 in the NB domain that might be critical for NLR function. Finally, we have shown that overexpression of *OsRLR1* leads to broad-range resistance with almost no penalty in terms of yield in rice.

Methods

Plant materials and growth conditions

The *rlr1* mutant was identified from a mutant library of the rice *indica* cultivar 'Jinhui 10' (JH10) generated by ethyl methane-sulphonate (EMS) treatment. For agronomic trait measurement, rice plants were grown in experimental fields in Chongqing, China, under natural conditions. For pathogen inoculation assays, rice plants were grown in a growth chamber (26 °C and under high-pressure sodium lamp) at Southwest University. All *N.*

benthamiana plants were grown in a greenhouse at the Rice Research Institute of Southwest University, Chongqing, China.

Pathogen inoculation and symptom assessment

At the four-leaf stage, plants in the growth chamber were spray-inoculated with a suspension of *P. oryzae* spores from three races (ZB7, ZB11 and ZB31) in 0.01% Tween-20 (1×10^5 spores/mL). Spores were obtained from *P. oryzae* races cultured on autoclaved sorghum seeds. At different time points after inoculation, leaves were excised for total RNA extraction. The length of diseased leaves and number of lesions on the leaf blade with the most serious disease symptoms of each plant were measured at 10 days post-inoculation (dpi).

At about 30 days old, plants grown in chamber were inoculated with the *Xoo* strain zhe173. Preparation of suspension and inoculation was performed as described previously (Peng *et al.*, 2008). After 5, 10 and 15 dpi, the lesion length was measured and bacterial growth was determined by counting colony-forming units (CFU) as described previously (Peng *et al.*, 2008). At booting stage, plants grown in field were inoculated with *Rhizoctonia solani* (RH-9) as described previously (Jia *et al.*, 2013).

Histological analysis

Staining with 3,3-diaminobenzidine (DAB) (Suolaibao) was conducted to detect H_2O_2 accumulation in leaves as described previously with slight modifications (Choi *et al.*, 2015). Briefly, leaves were detached and placed in DAB solution (10 mM MES, 1 mg/mL DAB) for 16 h, then cleared in alcohol. The leaves were examined with a stereomicroscope (SZX16/SZX10; Olympus, Japan). At the seedling stage, leaves of *T₀* plants transformed with *ProOsRLR1:GUS* were stained for about 12 h at 37 °C in β -glucuronidase (GUS) solution (Sigma). The stained leaf samples were used for paraffin sectioning. Sections were imaged using a Nikon Eclipse E600 microscope (Nikon, Japan).

Rice transformation

To generate the complementation and overexpression construct, the coding sequence of *OsRLR1* was amplified from JH10 and cloned into the digested pCA1300 vector containing a maize *Ubiquitin* promoter. Likewise, the coding sequence of *OsRLR1_M* was amplified from *rlr1* and cloned into pCA1300 vector with the same method. A 3484 bp (before start codon) promoter sequence of *OsRLR1* was amplified from JH10 and ligated to the digested pCA1300 vector to drive *GUS* expression. All primers used are listed in Table S1.

Transient expression assays in rice protoplasts

The vector pAN580 harbouring GFP under the control of $2 \times$ CaMV35S promoter was used for analyses of *OsRLR1* and *OsWRKY19* subcellular localizations in the rice protoplasts. The rice protoplasts were isolated following a method described previously (Ma *et al.*, 2017). The GFP and RFP fluorescence signals were observed using a confocal microscope (LSM800; Zeiss, Germany). Transient expression of the *LUC* reporter was achieved via the same method. The *Pro35S:Renilla-LUC* activity was measured as a control to normalize *LUC* activity among samples using a luminometer (GloMax; Promega, USA).

Yeast two-hybrid assay

Yeast two-hybrid assays were conducted with the Y2H Gold yeast strain using the GAL4 two-hybrid system (Clontech) following the manufacturer's instructions. The pGADT7 and pGBKT7 vectors

were used for plasmid constructions. Double dropout plates lacking Trp and Leu were used to select co-transformed colonies. Protein interactions were detected by measuring the growth of colonies on QDO plates lacking Trp, Leu, Ade and His but containing AbA (100 ng/mL).

Transient expression in *Nicotiana benthamiana* leaves

Agrobacterium tumefaciens strain GV3101 containing the target plasmid was grown in YEB medium with antibiotic selection to $OD_{600} = 0.6$ – 0.8 . Cells were suspended to an $OD_{600} = 0.4$ in MES buffer (10 mM $MgCl_2$, 10 mM MES; pH 5.6) and kept in the dark for 2–4 h before inoculation. Leaves were analysed at 2–3 days after transformation.

Bimolecular fluorescence complementation assays

OsRLR1 and *OsRLR1_M* (the mutated form of *OsRLR1*) were fused with the sequence coding the C-terminal fragment of the yellow fluorescent protein (cYFP) in the pxy104 vector. *OsWRKY19* was fused with the sequence coding the N-terminal portion of the yellow fluorescent protein (nYFP) in the pxy106 vector. *A. tumefaciens* strains containing the different plasmids were mixed prior to inoculation in *N. benthamiana* leaves. Leaves were stained with DAPI (Sigma) 1 h before examination with a confocal microscope.

Cell fractionation

A plant nuclear and cytoplasmic protein extraction kit (BestBio) was used to extract nuclear and cytoplasmic fractions from *N. benthamiana* leaves expressing *OsWRKY19-GFP* or *OsRLR1-GFP*, following the protocol provided by the manufacturer. The rabbit anti-GFP antibodies (Abcam) and anti-Rabbit IgG light-chain antibodies (Abcam) were used to detect the fusion proteins by Western blot.

Split luciferase assay

The 2 × CaMV35S promoter was used for expressing *OsRLR1-Cluc* or *OsRLR1_M-Cluc* with *OsWRKY19-Nluc* in *N. benthamiana*, respectively. The split luciferase assay was conducted as described before (Chen *et al.*, 2008). 1 mM luciferin was sprayed to the inoculated leaves before *LUC* activity was captured by CCD imaging camera (Lumina Series III; IVIS, USA).

Chromatin immunoprecipitation analysis

A ChIP assay was conducted using the EpiQuik Plant ChIP kit (EpiGentek) following the protocol provided by manufacturer with slight improvement. Leaf blades of the wild type and *rlr1* mutant were used for the ChIP assay. The rabbit anti-*OsWRKY19* polyclonal antibodies (the specific C-terminal 175–277 amino acid was purified from *E. coli* and injected into rabbit to get the antibodies) and pre-immune IgG (control) were used in protein/DNA immunoprecipitation. The total genomic DNA extract (input) and purified DNA eluent after IP were used in a qPCR assay.

Co-immunoprecipitation assay

Pro2 × 35S:*OsRLR1-Myc* or *Pro2* × 35S:*OsRLR1_M-Myc* was co-expressed with *Pro2* × 35S:*OsWRKY19-GFP* and P19 (a silencing inhibitor) in *N. benthamiana* leaves. Proteins were extracted from the agroinfiltrated *N. benthamiana* leaves with the extraction buffer (140 mM NaCl, 2.7 mM KCl, 25 mM Na_2HPO_4 , 1.5 mM KH_2PO_4 , 0.01 mM EDTA and 0.05% NP-40) supplemented with a protease inhibitor cocktail, PMSF (0.5 mM) and DTT (5 mM). 100 µL of extract after centrifugation at 13 000 rpm for 30 min was used

as input and the remainder was incubated with anti-mouse Myc antibodies (Abcam: Cambridgeshire, England, UK) or anti-mouse IgG antibodies (Abcam) at 4 °C overnight. The protein and antibody mixture was then incubated with agarose protein A beads at 4 °C for 4 h. The suspension was centrifuged at 1000g for 5 min, and the coimmunoprecipitate mixture was washed four times. The protein in precipitate and input were separated by SDS-PAGE and analysed by Western blot using GFP and Myc antibodies.

Acknowledgements

The authors are grateful to Prof. Yuxuan Hou and Song Liu from the China Rice Research Institute, Hangzhou Province, for kindly providing the Xoo strain. We thank Tongming Wang for his help in manuscript revision. This work was supported by grants from the National Key Transform Program (2016ZX08001-002), National Key Program for Research and Development (2017YFD0100201, 2017YFD0100202) and the Project of ChongQing Science & Technology Commission (cstc2018jcsx-msybX0250).

Conflicts of interest

Authors declare no conflict of interest.

Author contributions

Guanghua He and Dan Du designed the research. Dan Du and Xin Lu performed the subcellular location, and BiFC and Y2H analysis. Yadi Xing performed the map-based cloning and phenotype analysis. Yadi Xing performed the expression analysis of *OsRLR1*. Changwei Zhang designed the pathogen inoculation analysis. Linjun Cai, Han Yun and Dan Du performed the pathogen inoculation analysis. Qiuli Zhang, Yingying Zhang and Mingming Liu performed agronomy analysis. Dan Du, Yadi Xing and Xinlong Chen performed the vector construction. Guanghua He and Xianchun Sang performed the EMS study and identified the mutant. Yinghua Ling and Zhenglin Yang performed the planting of the materials in the field. Yunfeng Li performed protein alignment analysis. Benoit Lefebvre performed 3D structure construction of *OsRLR1* and revision of the manuscript. Dan Du and Changwei Zhang wrote the article.

References

- Bendahmane, A., Farnham, G., Moffett, P. and Baulcombe, D.C. (2002) Constitutive gain-of-function mutants in a nucleotide binding site-leucine rich repeat protein encoded at the Rx locus of potato. *Plant J.* **32**, 195–204.
- Boyce, D.C., Nam, J. and Dangel, J.L. (1998) The Arabidopsis thaliana RPM1 disease resistance gene product is a peripheral plasma membrane protein that is degraded coincident with the hypersensitive response. *Proc. Natl Acad. Sci. USA* **95**, 15849–15854.
- Cao, H., Glazebrook, J., Clarke, J.D., Volko, S. and Dong, X.N. (1997) The Arabidopsis NPR1 gene that controls systemic acquired resistance encodes a novel protein containing ankyrin repeats. *Cell* **88**, 57–63.
- Cao, H., Li, X. and Dong, X.N. (1998) Generation of broad-spectrum disease resistance by overexpression of an essential regulatory gene in systemic acquired resistance. *Proc. Natl Acad. Sci. USA* **95**, 6531–6536.
- Chen, X.W. and Ronald, P.C. (2011) Innate immunity in rice. *Trends Plant Sci.* **16**, 451–459.
- Chen, H.M., Zou, Y., Shang, Y.L., Lin, H.Q., Wang, Y.J., Cai, R., Tang, X.Y. *et al.* (2008) Firefly luciferase complementation imaging assay for protein-protein interactions in plants. *Plant Physiol.* **146**, 368–376.

- Cheng, H.T., Liu, H.B., Deng, Y., Xiao, J.H., Li, X.H. and Wang, S.P. (2015) The WRKY45-2 WRKY13 WRKY42 transcriptional regulatory cascade is required for rice resistance to fungal pathogen. *Plant Physiol.* **167**, 1087–1099.
- Chern, M., Fitzgerald, H.A., Canlas, P.E., Navarre, D.A. and Ronald, P.C. (2005) Overexpression of a rice NPR1 homolog leads to constitutive activation of defense response and hypersensitivity to light. *Mol. Plant Microbe In* **18**, 511–520.
- Choi, C., Hwang, S.H., Fang, I.R., Il Kwon, S., Park, S.R., Ahn, I., Kim, J.B. et al. (2015) Molecular characterization of *Oryza sativa* WRKY6, which binds to W-box-like element 1 of the *Oryza sativa* pathogenesis-related (PR) 10a promoter and confers reduced susceptibility to pathogens. *New Phytol.* **208**, 846–859.
- De Oliveira, A.S., Koolhaas, I., Boiteux, L.S., Caldararu, O.F., Petrescu, A.J., Resende, R.O. and Kormelink, R. (2016) Cell death triggering and effector recognition by Sw-5 SD-CNL proteins from resistant and susceptible tomato isolines to Tomato spotted wilt virus. *Mol Plant Pathol* **17**, 1442–1454.
- Devaiah, B.N., Karthikeyan, A.S. and Raghothama, K.G. (2007) WRKY75 transcription factor is a modulator of phosphate acquisition and root development in arabidopsis. *Plant Physiol.* **143**, 1789–1801.
- Dodds, P.N. and Rathjen, J.P. (2010) Plant immunity: towards an integrated view of plant-pathogen interactions. *Nat. Rev Genet* **11**, 539–548.
- Eulgem, T., Rushton, P.J., Robatzek, S. and Somssich, I.E. (2000) The WRKY superfamily of plant transcription factors. *Trends Plant Sci.* **5**, 199–206.
- Grant, M., Brown, I., Adams, S., Knight, M., Ainslie, A. and Mansfield, J. (2000) The RPM1 plant disease resistance gene facilitates a rapid and sustained increase in cytosolic calcium that is necessary for the oxidative burst and hypersensitive cell death. *Plant J.* **23**, 441–450.
- Grant, M.R., Godiard, L., Straube, E., Ashfield, T., Lewald, J., Sattler, A., Innes, R.W. et al. (1995) Structure of the Arabidopsis Rpm1 gene enabling dual-specificity disease resistance. *Science* **269**, 843–846.
- HammondKosack, K.E. and Jones, J.D.G. (1997) Plant disease resistance genes. *Annu. Rev. Plant Phys.* **48**, 575–607.
- Howles, P., Lawrence, G., Finnegan, J., McFadden, H., Ayliffe, M., Dodds, P. and Ellis, J. (2005) Autoactive alleles of the flax L6 rust resistance gene induce non-race-specific rust resistance associated with the hypersensitive response. *Mol. Plant Microbe In* **18**, 570–582.
- Hu, L., Wu, Y., Wu, D., Rao, W.W., Guo, J.P., Ma, Y.H., Wang, Z.Z. et al. (2017) The coiled-coil and nucleotide binding domains of BROWN PLANTHOPPER RESISTANCE14 function in signaling and resistance against planthopper in rice. *Plant Cell* **29**, 3157–3185.
- Inoue, H., Hayashi, N., Matsushita, A., Liu, X.Q., Nakayama, A., Sugano, S., Jiang, C.J. et al. (2013) Blast resistance of CC-NB-LRR protein Pb1 is mediated by WRKY45 through protein-protein interaction. *Proc. Natl Acad. Sci. USA* **110**, 9577–9582.
- Jia, Y., Liu, G., Park, D.S. and Yang, Y. (2013) Inoculation and scoring methods for rice sheath blight disease. *Methods Mol. Biol.* **956**, 257–268.
- Jones, J.D.G. and Dangl, J.L. (2006) The plant immune system. *Nature* **444**, 323–329.
- Kalder, M., Barth, M., Somssich, I.E. and Lippok, B. (2003) Members of the Arabidopsis WRKY group III transcription factors are part of different plant defense signaling pathways. *Mol. Plant Microbe In* **16**, 295–305.
- Li, W.T., Chern, M.S., Yin, J.J., Wang, J. and Chen, X.W. (2019) Recent advances in broad-spectrum resistance to the rice blast disease. *Curr. Opin. Plant Biol.* **50**, 114–120.
- Lolle, S., Greeff, C., Petersen, K., Roux, M., Jensen, M.K., Bressendorff, S., Rodriguez, E. et al. (2017) Matching NLR immune receptors to autoimmunity in camta3 mutants using antimorphic NLR alleles. *Cell Host Microbe* **21**, 518–529.
- Lukasik, E. and Takken, F.L.W. (2009) STANDING strong, resistance proteins instigators of plant defence. *Curr. Opin. Plant Biol.* **12**, 427–436.
- Ma, L., Sang, X.C., Zhang, T., Yu, Z.Y., Li, Y.F., Zhao, F.M., Wang, Z.W. et al. (2017) ABNORMAL VASCULAR BUNDLES regulates cell proliferation and procambium cell establishment during aerial organ development in rice. *New Phytol* **213**, 275–286.
- Mackey, D., Holt, B.F., Wiig, A. and Dangl, J.L. (2002) RIN4 interacts with *Pseudomonas syringae* type III effector molecules and is required for RPM1-mediated resistance in Arabidopsis. *Cell* **108**, 743–754.
- Maekawa, T., Cheng, W., Spiridon, L.N., Toller, A., Lukasik, E., Saijo, Y., Liu, P.Y. et al. (2011) Coiled-coil domain-dependent homodimerization of intracellular barley immune receptors defines a minimal functional module for triggering cell death. *Cell Host Microbe* **9**, 187–199.
- Mestre, P. and Baulcombe, D.C. (2006) Elicitor-mediated oligomerization of the tobacco N disease resistance protein. *Plant Cell* **18**, 491–501.
- Molla, K.A., Karmakar, S., Molla, J., Bajaj, P., Varshney, R.K., Datta, S.K. and Datta, K. (2020) Understanding sheath blight resistance in rice: the road behind and the road ahead. *Plant Biotechnol. J.* **18**, 895–915.
- Monosi, B., Wissner, R.J., Pennill, L. and Hulbert, S.H. (2004) Full-genome analysis of resistance gene homologues in rice. *Theor. Appl. Genet.* **109**, 1434–1447.
- Peng, Y., Bartley, L.E., Chen, X.W., Dardick, C., Chern, M.S., Ruan, R., Canlas, P.E. et al. (2008) OsWRKY62 is a negative regulator of basal and Xa21-mediated defense against *Xanthomonas oryzae* pv. *oryzae* in rice. *Molecular Plant* **1**, 446–458.
- Roberts, M., Tang, S.J., Stallmann, A., Dangl, J.L. and Bonardi, V. (2013) Genetic requirements for signaling from an autoactive plant NB-LRR intracellular innate immune receptor. *PLoS Genet.* **9**(4), e1003465.
- Sels, J., Mathys, J., De Coninck, B.M.A., Cammue, B.P.A. and De Bolle, M.F.C. (2008) Plant pathogenesis-related (PR) proteins: A focus on PR peptides. *Plant Physiol. Bioch.* **46**, 941–950.
- Shen, Q.H., Zhou, F.S., Bieri, S., Haizel, T., Shirasu, K. and Schulze-Lefert, P. (2003) Recognition specificity and RAR1/SGT1 dependence in barley Mla disease resistance genes to the powdery mildew fungus. *Plant Cell* **15**, 732–744.
- Shimono, M., Koga, H., Akagi, A., Hayashi, N., Goto, S., Sawada, M., Kurihara, T. et al. (2012) Rice WRKY45 plays important roles in fungal and bacterial disease resistance. *Mol. Plant Pathol.* **13**, 83–94.
- Shirasu, K. (2009) The HSP90-SGT1 chaperone complex for NLR immune sensors. *Annu. Rev. Plant Biol.* **60**, 139–164.
- Sukarta, O.C.A., Sloodweg, E.J. and Goverse, A. (2016) Structure-informed insights for NLR functioning in plant immunity. *Semin. Cell Dev. Biol.* **56**, 134–149.
- Sweat, T.A., Lorang, J.M., Bakker, E.G. and Wolpert, T.J. (2008) Characterization of natural and induced variation in the LOV1 gene, a CC-NB-LRR gene conferring victorin sensitivity and disease susceptibility in Arabidopsis. *Mol Plant Microbe In* **21**, 7–19.
- Swiderski, M.R., Birker, D. and Jones, J.D.G. (2009) The TIR domain of TIR-NB-LRR resistance proteins is a signaling domain involved in cell death induction. *Mol. Plant. Microbe. In* **22**, 157–165.
- Takken, F.L.W., Albrecht, M. and Tameling, W.I.L. (2006) Resistance proteins: molecular switches of plant defence. *Curr. Opin. Plant Biol.* **9**, 383–390.
- Tameling, W.I.L., Elzinga, S.D.J., Darmin, P.S., Vossen, J.H., Takken, F.L.W., Haring, M.A. and Cornelissen, B.J.C. (2002) The tomato R gene products I-2 and Mi-1 are functional ATP binding proteins with ATPase activity. *Plant Cell* **14**, 2929–2939.
- Tameling, W.I.L., Vossen, J.H., Albrecht, M., Lengauer, T., Berden, J.A., Haring, M.A., Cornelissen, B.J.C. and et al. (2006) Mutations in the NB-ARC domain of I-2 that impair ATP hydrolysis cause autoactivation. *Plant Physiol.* **140**, 1233–1245.
- Tang, J.Y., Zhu, X.D., Wang, Y.Q., Liu, L.C., Xu, B., Li, F., Fang, J. et al. (2011) Semi-dominant mutations in the CC-NB-LRR-type R gene, NLS1, lead to constitutive activation of defense responses in rice. *Plant J.* **66**, 996–1007.
- Tao, Y., Yuan, F.H., Leister, R.T., Ausubel, F.M. and Katagiri, F. (2000) Mutational analysis of the Arabidopsis nucleotide binding site-leucine-rich repeat resistance gene RPS2. *Plant Cell* **12**, 2541–2554.
- Tena, G., Boudsocq, M. and Sheen, J. (2011) Protein kinase signaling networks in plant innate immunity. *Curr. Opin. Plant Biol.* **14**, 519–529.
- Timilsina, S., Potnis, N., Newberry, E.A., Liyanapathirana, P., Iruegas-Bocardo, F., White, F.F., Goss, E.M. et al. (2020) Xanthomonas diversity, virulence and plant-pathogen interactions. *Nat. Rev. Microbiol.* **18**, 415–427.
- Tran, D.T.N., Chung, E.H., Habring-Muller, A., Demar, M., Schwab, R., Dangl, J.L., Weigel, D. et al. (2017) Activation of a plant NLR complex through heteromeric association with an autoimmune risk variant of another NLR. *Curr. Biol.* **27**, 1148–1160.

- van Loon, L.C., Rep, M. and Pieterse, C.M.J. (2006) Significance of inducible defense-related proteins in infected plants. *Annu. Rev. Phytopathol.* **44**, 135–162.
- Van Ooijen, G., Mayr, G., Kasiem, M.M.A., Albrecht, M., Cornelissen, B.J.C. and Takken, F.L.W. (2008) Structure-function analysis of the NB-ARC domain of plant disease resistance proteins. *J. Exp. Bot.* **59**, 1383–1397.
- Wang, Y.Y., Feng, L., Zhu, Y.X., Li, Y., Yan, H.W. and Xiang, Y. (2015) Comparative genomic analysis of the WRKY III gene family in populus, grape, arabidopsis and rice. *Biology Direct* **10**, 48.
- Wang, J.Z., Wang, J., Hu, M.J., Wu, S., Qi, J.F., Wang, G.X., Han, Z.F. et al. (2019) Ligand-triggered allosteric ADP release primes a plant NLR complex. *Science* **364**, 43.
- Wilson, R.A. and Talbot, N.J. (2009) Under pressure: investigating the biology of plant infection by *Magnaporthe oryzae*. *Nat. Rev. Microbiol.* **7**, 185–195.
- Xie, Z., Zhang, Z.L., Zou, X.L., Huang, J., Ruas, P., Thompson, D. and Shen, Q.J. (2005) Annotations and functional analyses of the rice WRKY gene superfamily reveal positive and negative regulators of abscisic acid signaling in aleurone cells. *Plant Physiol.* **137**, 176–189.
- Xing, Y.D., Du, D., Xiao, Y.H., Zhang, T.Q., Chen, X.L., Feng, P., Sang, X.C. et al. (2016) Fine Mapping of a New Lesion Mimic and Early Senescence 2 (Imes2) Mutant in Rice. *Crop Sci.* **56**, 1550–1560.
- Zhang, Y.L., Goritschnig, S., Dong, X.N. and Li, X. (2003) A gain-of-function mutation in a plant disease resistance gene leads to constitutive activation of downstream signal transduction pathways in suppressor of npr1-1, constitutive 1. *Plant Cell* **15**, 2636–2646.

Supporting information

Additional supporting information may be found online in the Supporting Information section at the end of the article.

Figure S1 Expression analysis of *OsRLR1*.

Figure S2 Phenotype and agronomic trait analysis of *OsRLR1*-OX plants.

Figure S3 Yeast two-hybrid assay between the same domains of *OsRLR1*.

Figure S4 Yeast two-hybrid assay between the AVR protein in *P. oryzae* and *OsRLR1*.

Figure S5 Localization of *OsWRKY19* and *OsRLR1* in the nucleus.

Figure S6 Relative expression level of *OsWRKY19*.

Figure S7 Agronomic traits in the wild type (WT), *rlr1* mutant, and *WRKY19*_{RNAi} plants.

Figure S8 Relative expression level of defence related genes after *P. oryzae* and *Xoo* inoculation.

Figure S9 Modelling of *OsRLR1* 3D protein structure.

Table S1 Primers used in this study.

Table S2 CLR proteins used in multiple sequence alignment.

Table S3 Mutated sites in NBS domain of other NLRs.